Large Eddy Simulation (LES) of a Steady Turbulent Flow over a Surface-Mounted Cube

Timothy Ganesan[C] and Mokhtar Awang

[1] *Department of Mechanical Engineering, Universiti Teknologi Petronas, Tronoh, 31750 Perak*, MALAYSIA

Abstract

The aim of this work is to simulate a steady turbulent flow over a surface-mounted cubicle obstacle using techniques in computational fluid dynamics (CFD). The simulation was done using an in-house code developed in the programming platform of Visual C++. The Finite Volume Method was used to compute numerically the solutions of the Navier-Stokes equation under turbulent conditions. The Quadratic Upstream Interpolation for Convective Kinetics (QUICK) numerical scheme was utilized with the Semi-Implicit Pressure Linked Equations (SIMPLE) as an algorithm. The code consists of a steady three-dimensional turbulent solver using the Large Eddy Simulation (LES) turbulent model. The simulated velocity flow profile is then compared against experimental data.

Keywords: : *Computational fluid dynamics; large eddy simulation;finite volume method; turbulence; Navier-Stokes equations*

1.   Introduction

Several works have been done analytically in search for the unique and smooth solution to the Navier-Stokes equations [1-3]. Large eddy simulation (LES) has been used in multiple studies to analyze turbulent flows in simple geometries and simple boundary conditions over the past twenty five years.

Prior to the nineties, any understanding of the major global features of flow patterns were based on flow visualization studies due to the absence of measurement data of three-dimensional flows around wall-mounted cubical obstacles. The first published work that contained measurement data of the turbulent velocity fields and energy balances around a surface-mounted cubical obstacle emerged in the nineties. Following this development, many experimental works were performed on a flow around a surface-mounted cubical obstacle in turbulent channel flows. Main features of the flow measurements describe the appearance of an arc-shaped vortex in the wake of the cube, horseshoe-type vortex at the windward face, flow separation at the top and side face of the cube and some vortex shedding downstream after the obstacle. These time-averaged flow features and experimental data of the flow characteristic is given in Hussein and Martinuzzi [4] and Nakamura *et al*. [5].

In recent five to ten years, LES has been applied to increasingly complex flows [6-9]. These researches mainly pioneered the idea of using the characteristics from the smallest resolved scales

---

[C] Corresponding Author: Timothy Ganesan
Email: tim.ganesan@gmail.com

to predict the subgrid scale (SGS) stresses. This idea then gave rise to the scale similarity model and the mixed model. This way, the required information from the smallest resolved scales were obtained mathematically by applying the filter operation twice. Bardina et al. [10] performed this method to rotating turbulent and to homogeneous isotropic flows. The follow-up from that work (Bardina et al. [10]) was carried out by Germano et al. [11], who then proceeded to develop the dynamic subgrid scale model. Computational works that involve the application LES for cases involving turbulent flow around cubic obstacle have been done in [12] and [13]. Similar works for these types of flow simulation using the LES model can be seen in [14-16].

In this work, a solver was developed using the finite volume method. The Quadratic Upstream Interpolation for Convective Kinetics (QUICK) numerical scheme (developed in [17]) was used with the Semi-Implicit Pressure Linked Equations (SIMPLE) algorithm. The Large Eddy Simulation (LES) static turbulent model developed in [18] was used to compute the subgrid scale (SGS) stresses. Many simple experiments have been done in the past to observe turbulent flow phenomenon and to outline its characteristics. In this paper, a three-dimensional steady turbulent flow phenomenon was simulated and compared against the experimental results by Matinuzzi and Tropea [19].

2. Mathematical Formulation and Computational Details

The mass flow rate across the faces of the fluid element is the product of density, area and the velocity component normal to the face. The gradient of the fluid velocities are as the following:

$$\frac{\partial \rho}{\partial t} + \frac{\partial (\rho u)}{\partial x} + \frac{\partial (\rho v)}{\partial y} + \frac{\partial (\rho w)}{\partial z} = 0 \tag{1}$$

where u, v and w are the velocity components in the x, y and z–direction respectively and ρ is the fluid density.

The momentum conservation principles are required in order to form a partial differential equation (Navier-Stokes). The solution to this partial differential equation would describe the behavior of the momentum in the flow. The final form of the momentum equation will be as the following:

$$\frac{\partial (\rho u)}{\partial t} + div(\rho uv) = div(\Gamma \cdot grad(u)) + S_u \tag{2}$$

where the $\partial(\rho u)/\partial t$ is the unsteady term, $div(\rho uv)$ is the convective term, $div(\Gamma \cdot grad u)$ is the diffusive term and S_u is the source term. The Γ in the diffusion term is the diffusion coefficient which is a function of the viscosity.

The LES model computes the subgrid scale stresses. Large eddies depend and extract energy from the bulk flow, their behavior is more anisotropic than small eddies (which are isotropic at high Reynolds number flows). A model such as the Reynolds Averaged Navier-Stokes (RANS) equations also describe the solution that comprises of the behavior of eddies in a time-averaged fashion. However, the LES model provides a means to compute a certain range of eddy scales (large eddies) through a statistical filtering procedure (spatial–averaging).

The filtering procedure is done by performing a convolution on the Navier-Stokes equation and the filter function (Gaussian filter, Fourier filter or the Tophat filter) producing the spatial-averaged Navier-Stokes equation. In this work, the Gaussian filter was applied. The convolution averages-off the small eddies (which effects are estimated using semi-empirical models called sub-grid scale (SGS) models) whereby computation is only done on the large eddies.

The LES model gives spatial-filtered Navier-Stokes equations:

$$\frac{\partial (\rho \overline{u}_i)}{\partial t} + div(\rho \overline{u}_i \overline{u}_j) = -\frac{\partial (\overline{p}_i)}{\partial x_i} + div(\Gamma \cdot grad \overline{u}_i) - \frac{\partial \tau_{ij}}{\partial x_j} \tag{3}$$

$$\tau_{ij} = \overline{\rho u_i u_j} + \rho \overline{u}_i \overline{u}_j \tag{4}$$

The terms $\overline{u}_i$ and $\overline{u}_j$ are the filtered velocities, $\overline{p}$ is the filtered pressure, the term τ_{ij} is the stress tensor that results from the statistical procedure (analogous to the Reynolds stresses in the RANS equations).

The LES Reynolds stresses arise due to the convective momentum transport which is a result of the interactions among SGS eddies per se and is modeled with a SGS turbulence model. The SGS turbulence model used in this computer code is the Smagorinsky-Lilly SGS model. The stresses C_{ij}, L_{ij} and R_{ij} are used together in the finite volume method and thus resulting in one SGS turbulence model which can be formulated as the following:

$$\tau_{ij} = -2\mu_{SGS}\overline{S}_{ij} + \frac{1}{3}\tau_{ii}\delta_{ij} \tag{5}$$

where μ_{SGS} is the artificial or the sub-grid scale viscosity which acts as the constant of proportionality and $\overline{S}_{ij}$ is the average strain rate . The size of the SGS eddies are determined by the filter choice as well as the filter cut-off width which is used during the averaging operation. The SGS viscosity can be obtained by the following semi-empirical formulation:

$$\mu_{SGS} = \rho\left(C_{SGS}\Delta\right)^2\left|\sqrt{2\overline{S}_{ij}\overline{S}_{ij}}\right| \tag{6}$$

where Δ is the filter cut-off width and is an C_{SGS} empirical constant which is usually specified in a range, $0.19 < C_{SGS} < 0.24$.

Due to the reduction in the turbulent scale in the three directions at the near-wall regions, the need for the usage of a wall functions. In this work, a simple two layer log-law based approximation was used at the near-wall regions (which consist of a viscous sub layer and a turbulent layer) [20]. No perturbation was introduced in the mean flow for turbulence generation. The constant velocity and static pressure boundary conditions (non-periodic) are defined in the spanwise direction at the inlet grids.

3. Description of Experiment

The experimental data performed by Matinuzzi and Tropea [19] was compared against the simulation results. The fluid used in this experiment was water (incompressible flow) with the density of 1000 kg/m^3 and viscosity of 0.001 kg/ms. The experiment was performed in a rectangular channel with a single cubicle obstacle mounted on the surface of the channel (internal flow). The Reynolds number (which is based on the channel height) was 12000 with the inlet velocity of 0.467 m/s.

The experiment was conducted at atmospheric pressure. The length (*x*-direction), height (*y*-direction) and width (*z*-direction) are 1.6m, 0.16m and 1.0m respectively. The obstacle was mounted at 0.8m from the inlet (*x*-direction) and 0.46m in the *z*-direction. This experiment was performed in a fully developed turbulent channel flow. The cubicle obstacle was placed at 5 times the channel height from the inlet (*x*-direction) and at the centerline of the width (*z*-direction). A detailed description of the experimental technique can be found in [21].

4. Solver parameters

In this work, the computational domain used is similar to the experimental design, at which the points where the experimental measurements are taken identical to the computational grid.

Prior to execution of the numerical solver, a number of parameters are required to be specified. These parameters are the numerical coefficients that are employed in the numerical scheme and the algorithm. These parameters influence the number of iterations, computational time, stability of computations and the convergence rate. The parameter types and the values that are used in this work can be summarized in Table 1:

TABLE I. INITIALIZED SOLVER PARAMETERS

Properties	Values
Iterations for velocity and pressure	3496
Relaxation factor for velocity	0.9
Relaxation factor for pressure	0.9
Convergence criterion for pressure correction matrix	1%
Mesh size (x, y, z) in (meters)	(0.032 ,0.05, 0.04)
SGS Constant, C_{SGS}	0.2

5.   Results Analysis

The velocity distributions obtained by the solver is compared with that obtained from the experiment. For the purpose of comparison, the most significant velocity gradients that influence the flow behavior are taken. To identify the significant velocity gradients, a scaling argument was used. From the analysis, the velocity gradients, $\partial u / \partial y$ was identified as the most significant term for the given dimensions of the setup and the flow conditions. Thus, the u-velocities (streamwise velocities) are taken with respect to the y-axis at different points in the x-direction.

The algorithms used in this work were programmed using C++ programming language on a personal computer with an Intel dual core processor running at 2 GHz. The overall CPU time taken for stabilization and convergence of the computations are approximately 3.2295 minutes.

The velocity distributions in the experimental results are normalized to the inlet velocity that is U/U_O. Similarly the distances in the experimental results are also normalized to the height of the obstacle which is respectively *x/H, y/H,* and *z/H.*

Seven sets of experimental results of the u-velocity distributions are obtained throughout the test section. Four sets of velocity distributions are used in the comparison at the region before the obstacle, one set right above the obstacle and two sets at the flow after the obstacle (the dissipation region). The normalized distances in the *x*, *y* and *z* -direction (*x/H, y/H,* and *z/H*) is at (0, 0, 0) is right above the obstacle. The following are the first four sets of velocity distributions which are taken for comparison. These sets are taken at the upstream region before the obstacle at *x/H* = -5, *x/H* = -2, *x/H* = -0.75 and *x/H* = -0.25.

The computed streamwise velocities when compared with the experimental data at the near-wall region are seen to have deviations (Figure 1 and 2). It can be seen that the usage of non-uniform grid produces more realistic results than a uniform grid for such cases. In [22] finer was used grid at the near-wall region. The simulations produced more accurate results as compared to the calculation done with a uniform grid which can be observed in [23]. Similar to [23], this work used a uniform grid which may be one of the reasons for inconsistencies mentioned above.

In Figure 3 and 4, it can be observed that the simulation results produce a qualitatively similar trend as compared with that of the experiment. However, the velocity profile produced by the simulation appears to have slight irregularities ('wiggles'). Similar occurrences have been observed in [24] while performing LES simulation on flow over a bluff body. In [25], it was stated that these wiggles can be attributed to a combination of two factors, the coarseness of the mesh and the numerical scheme applied. In [24] also experienced these similar wiggles in the streamwise velocities in their simulation. Therefore, in [25], it was suggested that a finer grid and a better

numerical scheme may produce smoother trend in the streamwise velocities and hence eliminate these wiggles.
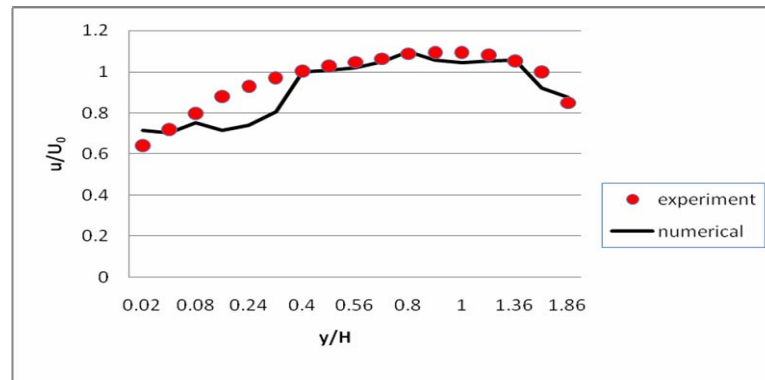
Figure 1: Comparison of velocity distributions at *x/H* = -5.
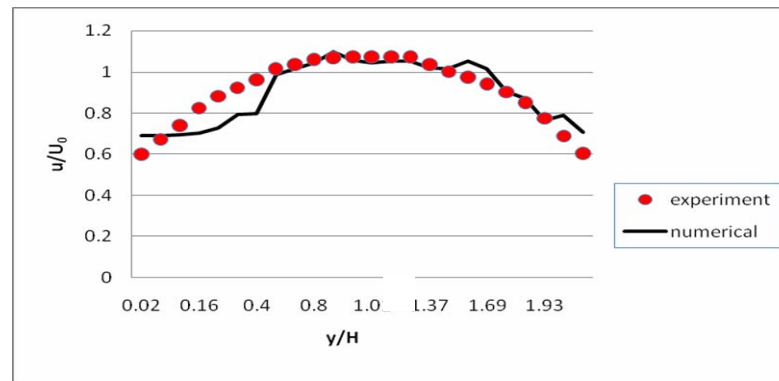
Figure 2: Comparison of velocity distributions at *x/H* = -2.
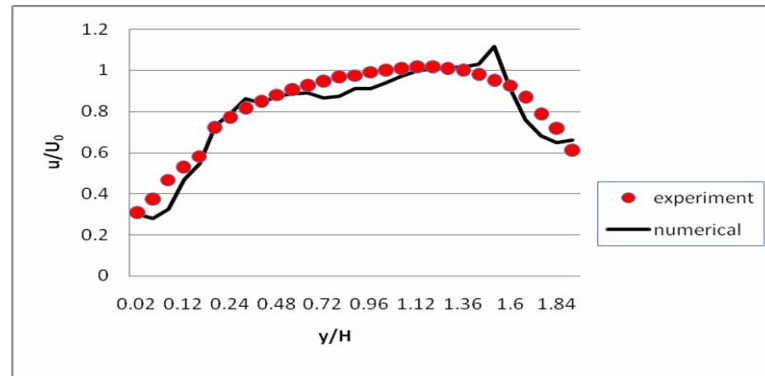
Figure 3: Comparison of velocity distributions at *x/H* = -0.75.

The solver had difficulty in accurately computing the flow behavior at the recirculation region (see Figure 6). This may be attributed to the inability of the SGS model (Smagorinsky model) to compute accurately the SGS stresses that heavily influences the flow during the recirculation phenomenon. One method to enhance the SGS model's accuracy is to modify it by including approximate boundary conditions. This was done in [26] where this method was stated to improve the accuracy of the computed SGS stresses. Another method was proposed in [27] where a new parameter was introduced and was said to improve the accuracy of the Smagorinsky model.

Besides, there are also slight inconsistencies for the velocities at the recirculation and the recovery region (refer to Figures 6 and 7). To trace the vortex, the vortex centre can be used where the velocity is zero. In this work, it can be observed that dissipation occurs gradually downstream after the obstacle or the step. Hence heading further downstream the vortex structure disappears which is consistent with the physical data.
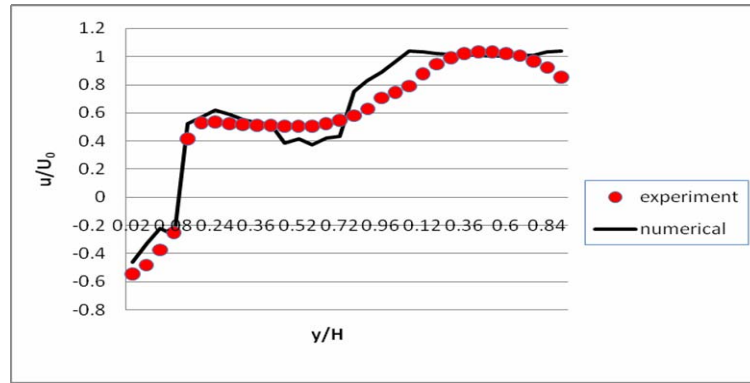
Figure 4: Comparison of velocity distributions at *x/H* = -0.25.

The following are the velocity distributions which are taken right above the obstacle (at *x/H* = 0) and at the flow after the obstacle (the dissipation region at *x/H* = 2 and *x/H* = 3).
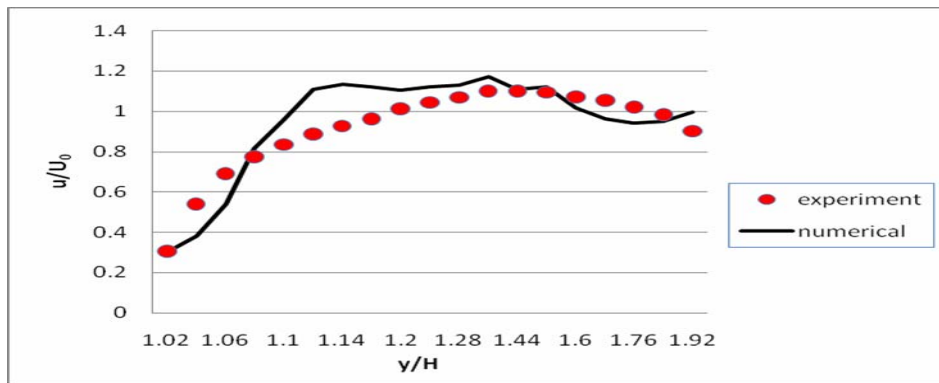
Figure 5: Comparison of velocity distributions at *x/H* = 0.

Beside the LES method, the RANS approach has also been seen to predict the re-attachment length, flow structure features and dissipation characteristics although at the expense of increased computational time (see [28] and [29]). The Quasi-DNS (QDNS)[30] was also proved to simulate flows around surface mounted obstacles very accurately. However the contributions of the SGS model in this scenario is very small. Although the QDNS method is very effective, if this method is used for cases with more complex geometry and higher turbulence levels, it would have very high computational costs (see [30]).

A similar work on identifying vortex dissipation downstream of flows was done in [31]. The dynamic Smagorinsky model (DM model) was also stated to give more realistic results as compared with the static Smagorinsky model.
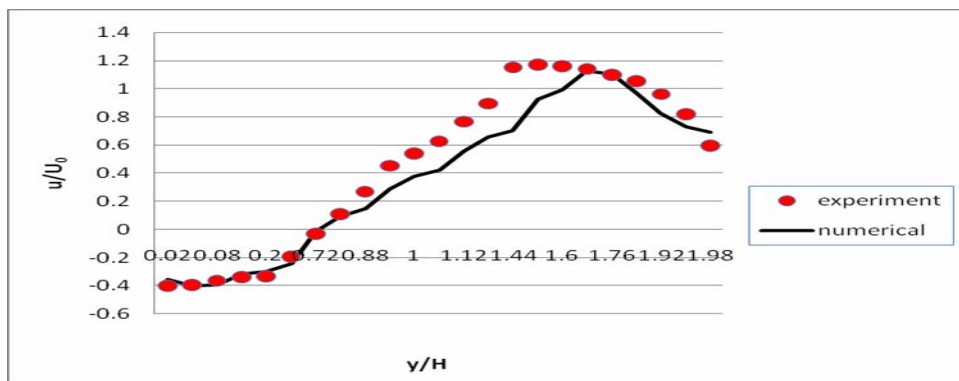
Figure 6: Comparison of velocity distributions at *x/H* = 2.

6
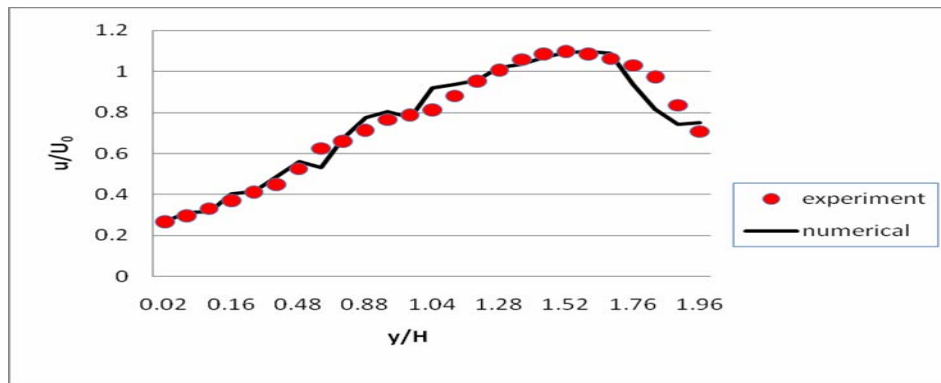
Figure 7: Comparison of velocity distributions at *x/H* = 3.

6. Error Analysis

The error in percentage (%) between the velocity distributions obtained by the numerical solver and the experimental results was computed using the following formulation:

$$error \ (\%) = \left| \frac{u - u'}{u'} \right| \times 100\% \tag{9}$$

where *u'* is the velocity obtained by the experimental results and *u* is the velocity obtained by the numerical solver.

The average error obtained for the four sets of velocity distributions are as the following: As the flow approaches the obstacle, the average error is observed to increase. The average error at *x/H* = -0.25 which is right before the obstacle is the highest at 15.545 %. This may be attributed to flow reversal, as could be observed in Figure 4 (negative velocity values) when the fluid encounters the mounted-obstacle. This phenomenon is not accurately captured by the numerical solver and hence results in higher error values. The average error in the velocity distribution is observed to reduce as compared with that in the flow reversal region in front of the obstacle. This may be explained by the fact that the flow above the obstacle exhibits comparatively higher stability as the mean flow direction is preserved. The average error at *x/H* = 2 has a higher value of 19.14% due to inability of the numerical solver to capture the finer details of the flow recirculation phenomenon. Finally at *x/H* = 3, is can be observed that the average error reduces again during flow recovery. Thus the solver computes the velocity profile with fair accuracy. The average error distribution in the streamwise direction can be seen in Figure 8.
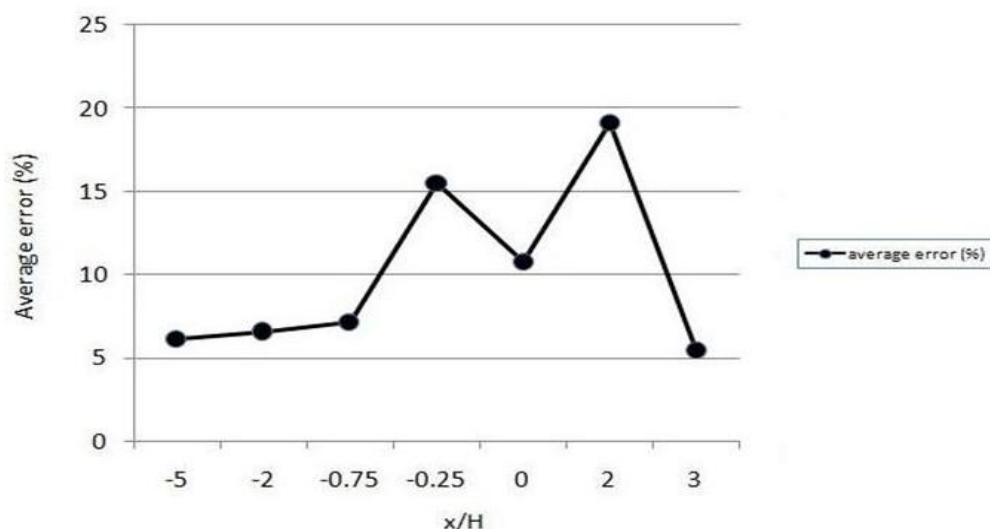
Figure 8: The average error distribution in the streamwise direction.

7.   Conclusions

Based on the analysis performed it can be concluded that the results produced by the simulation are fairly consistent with the experimental results. Although the in-house source code equipped with the LES turbulence model is complete, further advancement and validation with empirical results with different flow conditions are necessary. Besides, vigorous grid independence studies needs to be conducted to produce more reliable computational results.

For instance, the numerical scheme of the solver can be upgraded to third order QUICK or other UPWIND schemes to cut down the approximation errors during numerical operation. Besides that, based on recent work [16] the static Smagorinsky model in this solver can be upgraded to the Dynamic Smagorinsky model to accurately capture the flow fluctuations due to turbulence. The option for more meshing techniques can also be included as one of the features in the solver. These upgrades and testing will increase the capacity of the simulator to solve a greater variation of flow cases with optimum accuracy.

Acknowledgements

References

[1]   El-Sayed A., *Fractional-order diffusion-wave equation*, Int. J. Theory Phys., **35**, 1996, pp. 311-322.

[2]   Huang F., and Liu F., *The time fractional diffusion equation and fractional advection-dispersion equation,* ANZIAM J., **46**, 2005, pp. 1-14.

[3]   Huang F., and Liu F., *The fundamental solution of the space-time fractional advection-dispersion equation,* J. Appl. Math. & Computing, **18**(1-2), 2005, p. 339-350.

[4]   H. Hussein and R. Martinuzzi, *Energy balance for turbulent flow around a surface mounted cube placed in a channel*. Phys. Fluids, **8** 3 1996, pp. 764–780

[5]   H. Nakamura, T. Igarashi and T. Takayuki, *Local heat transfer around a wall-mounted cube in the turbulent boundary layer*. Int. J. Heat Mass Transfer, **44,** 2001, pp. 3385–3395

[6]   O. Metais, M. Lesieur, *Statistical predictability of decaying turbulence*, J. Atmos. Sci. **43** 1986, pp. 857–870.

[7]   A. Yakhot, S.A. Orszag, V. Yakhot, M. Israeli, *Renormalization group formulation of large eddy simulation*, J. Sci. Comput. **4** ,1989, pp 139–158.

[8]   M. Germano, *Turbulence, the filtering approach,* J. Fluid Mech. **238**,1992, pp 325–336.

[9]   Moin, P., and Jimenez, J., *Large Eddy Simulation of complex trubulent flows*, AIAA, pp 93-3099, 1993, Orlando, Florida.

[10]   Bardina, J., Ferziger, J.H. & Reynolds, W.C , *Improved turbulence models based on large eddy simulation of homogeneous, incompressible turbulent flows*,   Report TF-19, Thermosciences Division, Dep. of Mech. Eng., 1983, Stanford University, Stanford Calfornia.

[11]   Germano, M., Piomelli,s U., Moin, P. & Cabot, W.H., *A dynamic subgrid scale eddy viscosity model*, Physc. Fluids A. **3** (7), 1991.

[12]   Shah K.B. and Ferziger J.H., *A fluid mechanicians view of wind engineering: large eddy simulation of flow past a cubic obstacle*, J. Wind Eng. Ind. Aerodyn. 67&68, 1997, pp 211–224.

[13]   Rodi W., Ferziger J.H., Breuer M., Pourquie M., Status of large eddy simulation: results of a workshop, ASME J. Fluids Eng. **119**, 1997, pp 248–262.

[14] SiniÏsa Krajnovi´c and Lars Davidson, *Large Eddy Simulation of the Flow Around a Bluff Body*, AIIA Journal, **4**(5), 2002, U.S.

[15] Krajnovi´c, S., and Davidson, L., *Large Eddy Simulation of the Flow Around a Three-Dimensional Bluff Body*, AIAA Journal, 2001, U.S.

[16] Krajnović S. and Davidson L., *Large-eddy simulation of the flow around a surface-mounted cube using a dynamic one-equation subgrid model*, 1999. Banerjee, J. Eaton, Editors , *The First Int. Symp. on Turbulence and Shear Flow Phenomena*, Beggel House, Inc., 1999, New York.

[17] Leonard B.P., *A Stable and Accurate Convective Modeling Procedure Based on Quadratic Upwind Interpolation*, Comp. Methods Appl. Mech. Eng. **19**, 1979, pp. 59 – 98.

[18] Smagorinsky J., *General Circulation Experiments with the Primitive Equations I. The Basic Experiment*, Monthly Weather Rev. **91**(3), 1963, p.99-164.

[19] Martinuzzi R. & Tropea C., *The flow around surface-mounted, prismatic obstacles placed in a fully developed channel flow*, Journal of Fluid Engineering, **11**, 1993, pp. 85.

[20] Schlichting H., Gersten K., *Boundary Layer Theory*. 8th revised and enlarged edition, Springer, New York, 2000, pp 522-525.

[21] Dimaczek G., Tropea C., Wang A.B., *Turbulent Flow Over Two-Dimensional, Surface-Mounted Obstacles: Plane and Axisymmetric Geometries*, 2nd European Turbulence Conference, Berlin, 1988.

[22] Arnal M., and Friedrich, R., On the effects of spatial-resolution and subgrid scale modelling in large eddy simulation of a recirculating flow. Proc. of the 9th GAMM-Conf. on Num. Methods in Fluid Mech. Lausanne, 1991.

[23] Friedrich, R. and Arnal, M., *Analyzing turbulent backward-facing step flow with the low-pass filtered Navier-Stokes equations*. Journal of Wind Eng. And Indutrial Aerodynamics. **35**, 1990, pp. 101-128.

[24] SiniÏsa Krajnovi´ and Lars Davidson, *Large Eddy Simulation of the Flow around a Bluff Body*, AIAA Journal, **40**(5), 2002.

[25] Krajnovi´ S., and Davidson L., *Large-Eddy Simulation of the Flow Around a Ground Vehicle Body*, Society of Automotive Engineers, SAE Paper 2001-01-0702, 2001.

[26] Morinishi, Y. & Kobayashi, T., *Large eddy simulation of backward-facing step flow*. International Symposium of Eng. Turbulence Modelling and Measurement. Dubrovnik, Yugoslavia, 1990.

[27] Yoshizawa. A., *Subgrid scale modelling with a variable length scale*. Physics of Fluids A.1, **7**, 1989, p.1293-1295.

[28] Iaccarino, G., Ooi, A., Durbin, P.A. and Behnia, M. *Reynolds averaged simulation of unsteady separated flow*, Int. J. Heat Fluid Flow, **24**, pp 147-156 (2003).

[29] Rodi, W., *Comparison of LES and RANS calculations of the flow around bluff bodies*, J. of Wind Eng. and Ind. Aerodynamics, **69**, pp 55-75 (1997)

[30] Farhadi, M. and Rahnama, M., *Large Eddy Simulation of Separated Flow over a Wall-Mounted Cube*, International Journal of Science and Technology (SCIENTIA IRANICA), **13**(2), pp. 124-133, 2006.

[31] Roquemore W.M., Chen L., Goss L.P. and Lynn W.F., *Joint US-France Workshop on Turbulent Reacting Flows*, Rouen, France, 1987.